10.2478/msr-2014-0008

MEASUREMENT SCIENCE REVIEW, Volume 14, No. 1, 2014

Generating Sub-nanometer Displacement Using Reduction Mechanism Consisting of Torsional Leaf Spring Hinges

Makoto Fukuda, Masato Hayashi, Sintaro Marita

Graduate School of Science and Technology, Hirosaki University, 3 Bunkyo-cho, Hirosaki-city, Aomori Pref. 036-8561, Japan, e-mail: fukuda@cc.hirosaki-u.ac.jp

Recent demand on the measurement resolution of precise positioning comes up to tens of picometers. Some distinguished researches have been performed to measure the displacement in picometer order, however, few of them can verify the measurement performance as available tools in industry. This is not only because the picometer displacement is not yet required for industrial use, but also due to the lack of standard tools to verify such precise displacement.

We proposed a displacement reduction mechanism for generating precise displacement using torsional leaf spring hinges (TLSHs) that consist of four leaf springs arranged radially. It has been demonstrated that a prototype of the reduction mechanism was able to provide one-nanometer displacement with 1/1000 reduction rate by a piezoelectric actuator. In order to clarify the potential of the reduction mechanism, a displacement reduction table that can be mounted on AFM stage was newly developed using TLSHs. This paper describes the design of the reduction mechanism and the sub-nanometer displacement performance of the table obtained from its dynamic and static characteristics measured by displacement sensors and from the AFM images.

Keywords: Sub-nanometer displacement, reduction mechanism, torsional leaf spring hinge, displacement standard, AFM verification.

1. INTRODUCTION

RECENT IMPROVEMENT of the positioning accuracy is distinguished due to the improvement of the resolution and the processing rate of the laser interferometer measurement system. However, the demand on the measurement resolution in future positioning is expected up to tens of picometers especially in the semiconductor industries. Such highly precise resolution in displacement measurement is difficult to realize not only because the order is beyond the resolution limit of the laser interferometer, but also due to the lack of standard tools that can generate picometer displacement to verify such precise resolution. There are few works on the instruments that can measure the several ten-picometer displacements. Nakata el al. proposes a displacement measurement instrument that has 40-picometer sensitivity using photonic crystal optics for interferometer [1]. There are several other works to carry out picometer measurement that uses the atomic lattice spacing as a reference of positioning [2]-[4]. Aketagawa et al. had important trials in which the lattice spacing of HOPS (highly oriented pyrolytic graphite) was used as a reference for a double-tunneling-probe STM (DTP-STM) of two-dimensional encoder scale with tens of picometer resolution [2], but the measurement apparatus itself is too complex to use as the picometer displacement generating tool.

As a precise displacement generator, we proposed a displacement reduction mechanism using torsional leaf spring hinges (TLSHs) that consist of four leaf springs arranged radially [5]. It has been demonstrated that the reduction mechanism was able to provide one-nanometer displacement with 1/1000 reduction rate for the sinusoidal, triangular and rectangular motions by a piezoelectric actuator.

This reduction mechanism has a potential to reduce the displacement up to several ten picometers because of the linearity of the TLSHs due to its lower stress concentration than flexure hinges. Then, in order to verify sub-nanometer positioning of the mechanism, a displacement reduction table that can be mounted on an AFM instrument is newly developed using the TLSHs. This paper describes the dynamic and static characteristics of the table measured by capacitance displacement sensors and the results of its positioning ability obtained from AFM images.

2. DISPLACEMENT REDUCTION TABLE USING TLSH

A displacement reduction table is so designed that the mechanism can be mounted on an AFM instrument, which is an S-image by Hitachi High-Tech Science Technologies Corporation [6], and that the reduction rate becomes less than 1/150, which can generate less than 10 pm of the displacement at the end table with a 1-nm input by a piezoelectric actuator.

The key element in this reduction mechanism is a torsional leaf spring hinge (TLSH), which consists of two plates supported by 4 leaf springs as shown in Fig.1.a). As the four leaf springs are independent of each other, the deformation of the leaf spring is induced by the addition of the deflection and torsion of the leaf spring while the two plates are twisted opposite each other. This structure has an advantage of being able to provide both the strong deflection stiffness and the sensitive torsional stiffness. Fig.1.b) shows a photograph of TLSHs where two TLSHs are machined from one block of SUS304.

A TLSH is employed as the fulcrum of a lever in the reduction mechanism. Fig.2.a) and 2.b) show the reduction mechanism consisting of four TLSHs and four levers. The bottom plates of TLSHs are able to be mounted on a base plate, and the top plates are connected with the levers. The base plate can be set on the AFM stage by magnetic force. The input force to TLSH is exerted in the circumference

direction by a piezoelectric actuator with a feedback of a strain gauge [7] and rotates the TLSH and the output deformation also comes up in the circumference direction with the reduction rate of the distances from the TLSH's center to the effort points of the input and the output forces. Each lever is pushed to the circumference direction by a steel ball in order to avoid the deformation due to the lever expansion.

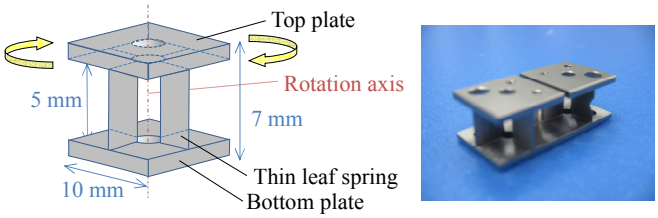

Fig.1. a) Structure of torsional leaf spring hinge
b) Photograph of a pair of TLSHs.

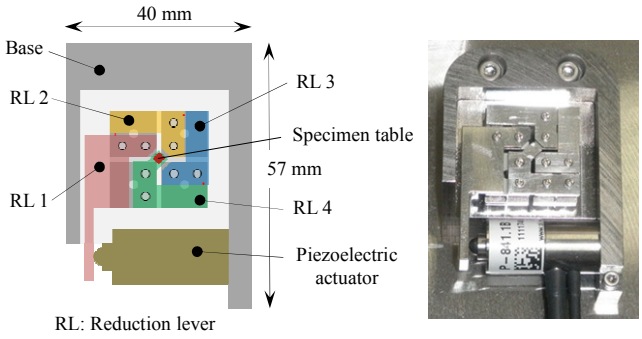

Fig.2. a) Structure of displacement reduction table that can be mounted on AFM stage, b) Photograph of the table.

The total reduction rate K is as follows:

$$\mathbf{K} = \frac{4}{26.5} \times \frac{4}{15} \times \frac{4}{15} \times \frac{5.5\sqrt{2}}{15} = \frac{1}{180} \qquad (1)$$

where the numerator and the denominator show the distance of the output and the input levers, respectively. The fractions show the reduction rate of each TLSH. The reason that the reduction rate of the 1st TLSH is smaller than that of the others is both to take sufficient length for the piezoelectric actuator and to twist the TLSH easily.

3. Experimental Setup

As measuring the displacement of the specimen table directly is difficult due to the table size and its location in the reduction mechanism center, an extension beam is used for the measurement. The extension beam is so mounted on the 4th TLSH that the midpoint of the beam is coincident with the center of the 4th TLSH. The displacement of the specimen table is expanded at the rate of 7 times. A schematic chart and a photograph of the setup are shown in Fig.3.a) and 3.b), respectively. In this setup, the input displacement induced by a piezoelectric actuator and the output displacement at two ends of the beam can be measured by capacitance displacement sensors: CDS1, CDS2, CDS3. The reduction mechanism is mounted on a silicone gel vibration isolator.

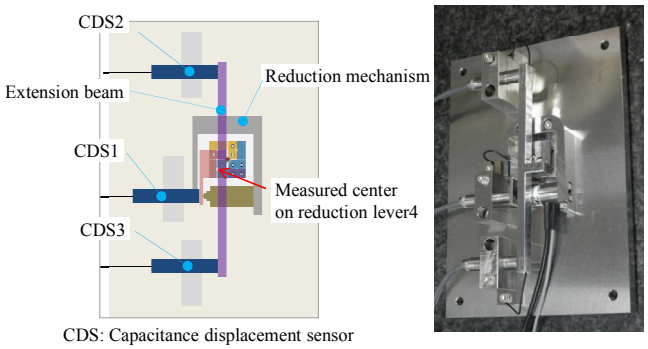

Fig.3. a) Measurement setup, b) Photograph of the setup.

4. Experimental Results

A. Dynamic Characteristics

Fig.4. shows the results of the transfer function from the input to a piezoelectric driver to the output of the capacitance displacement sensor (CDS 2) at an end of the extension beam. The input and the output voltages are 1.5 V and 0.316 V, respectively, which correspond to the input and the output displacements of 1500 nm and 75 nm, respectively. Red and blue lines show the gain and the phase of the transfer function. The setup has anti-resonance and resonance frequencies at 145 Hz and 350 Hz, respectively. As this resonance frequency includes the mass of the extension beaming, the actual resonance frequency at the specimen table may be higher than 350 Hz.

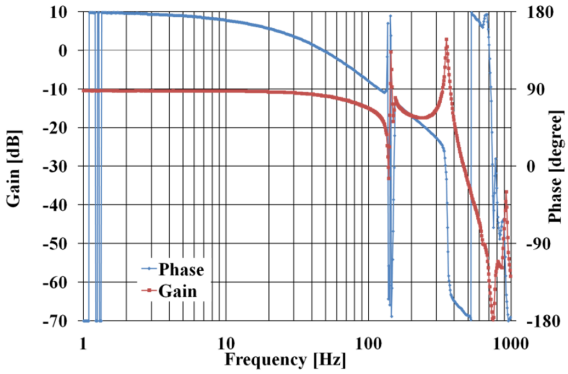

Fig.4. Transfer function from the input to a piezoelectric actuator to the output of capacitance sensor CDS2. Red and blue lines show gain and phase, respectively.

B. Static Characteristics

The input and output displacements obtained by the capacitance displacement sensors for various amplitudes of triangle signals are shown in Fig.5.a), 5.b) and 5.c). The input amplitudes are 1500 nm, 150 nm and 15 nm for Fig.5.a), Fig.5.b) and 5.c), respectively.

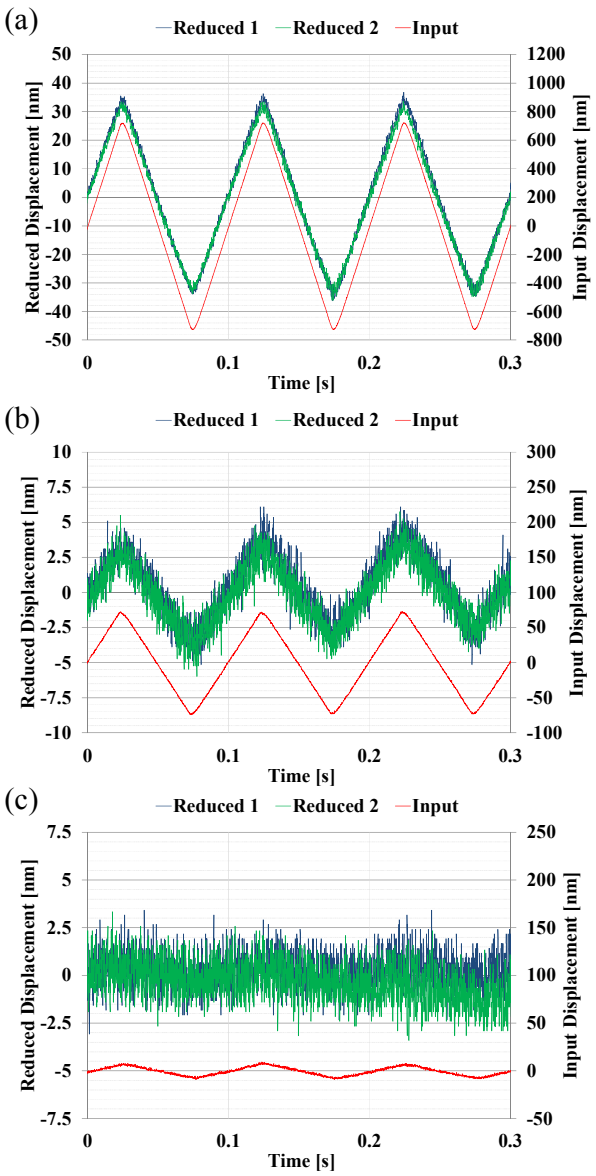

Fig.5. Measured displacements by capacitance sensors. Red, blue and green lines are at piezoelectric actuator, at extension beam CDS2 and CDS3. a) input amplitude: 1500 nm, b) 150 nm and c) 15 nm.

Red lines show the input displacement at right-hand co-ordinate y axis, green and blue lines show the output displacement through the reduction mechanism and the extension beam at left-hand co-ordinate y axis. The amplitudes of the input, the outputs of the capacitance sensors CDS2 and CDS3 and the displacement at the specimen table, which is calculated from the measured output displacement, are shown in Table 1. The reduction rate from the piezoelectric actuator input to the capacitance sensor outputs was 1/23. This rate was smaller than the one designed as 1/25. The total reduction rate was calculated as 1/165, which is smaller than the one designed as 1/180 because the capacitance sensors should be set on the inward side.

Table 1. Displacement amplitudes of the input to piezoelectric actuator, the output of extension beam and the specimen table of the reduction mechanism under conditions in Fig.5. a), b), c)

	(a)	(b)	(c)
Input amplitude	1500 nm	150 nm	15 nm
Output amplitude at CDS2	66 nm	6.6 nm	0.73 nm
Output amplitude at specimen table	9.17 nm	0.917 nm	0.101 nm

C. AFM IMAGING

Mica is relatively stable in air as compared with such as Si substrate, which is easily oxidized, and it is easy to get a new atomic plane as the cleavage plane. The atomic image of mica can be obtained by the AFM measurement mode of the SPM (Scanning Probe Microscope) instrument. We compare the obtained images by using both the shape images and the friction images. The observation area of the obtained image was 10-nm^2.

First, we compared the atomic image with and without the reduction mechanism. The results are shown in Fig.6.a) to 6.d). As shown in the AFM images of the mica specimen only (Fig.6.a) and 6.b)), namely without the reduction mechanism, it was possible to observe the atomic image as relatively accurate and the pitch between the atoms was measured as 0.55 nm which is nearly the ideal pitch of 0.52 nm [8]. However, it was difficult to obtain the ideal atomic images in the AFM observation for the mica specimen mounted on the specimen table of the reduction mechanism. As shown in Fig.6.c) and 6.d), obtained AFM images have thin lines in horizontal in both the shape and friction images. The reasons for this can be considered to be both the thermal fluctuation and the natural frequency of the reduction mechanism. However, periodic diagonal lines, whose period is 0.45 nm, can be observed in both figures.

The measurement was carried out at room temperature of 23±0.5□in the cyclic period of 2 hours. The scanning period was 5 Hz for 256 lines for 10 nm x 10 nm area. This means it will take around 52 s to measure the sample that comes to the temperature fluctuation of 1/120 K during the measurement. The reduction mechanism was so devised that each lever was pushed to the circumference direction by a small steel ball in order to avoid the longitudinal expansion of the lever. The most influenced size is estimated as 15 mm. Therefore, 15(mm)*10^-5(1/K)*1/120(K) = 1.25 nm in total fluctuation due to thermal circumstance. The cantilever type was SI-AF10, whose top curvature R < 10 nm.

On the other hand, the natural frequency of the reduction mechanism at 350 Hz has an acute peak and becomes larger than 0 dB as shown in Fig.4. This has a possibility to increase the vibration during the measurement. It is possible, in principle, to obtain the shifted atomic images when the specimen table moves in rectangular because the response time of the table is fast enough to settle the table, less than 0.004 s as shown in Fig.5.

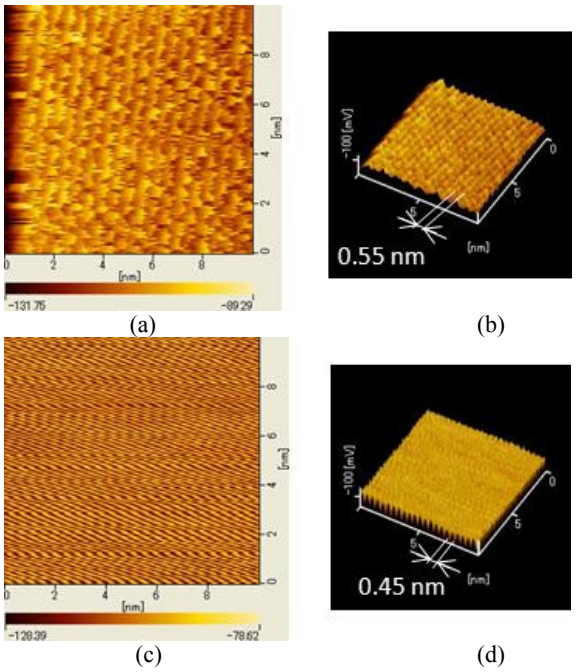

Fig.6. Mica AFM images observed by shape and friction modes. a) and b) shape and friction modes of mica on AFM stage, c) and d) shape and friction modes of mica on the reduction table mounted on AFM stage.

AFM images obtained during the table motion with and without the rectangular waves are shown in Fig.7.a) and b). In Fig.7.b), the input amplitude and frequencies of the rectangular wave were 90 nm and 0.3 Hz, which correspond to 0.75-nm displacement on the specimen table when the reduction rate of the mechanism was 1/180. AFM probe scanning frequency was kept constant at 10 Hz. The pixels in x and y direction were 512 and 256, respectively. The rectangular step changes were given at each position where the color changed. It can be seen that the period change in the atom images occurred at the rectangular step change of the specimen table. The reason for changing the color of the AFM image is possibly that the specimen table moves not only in horizontal but also in vertical direction when the table moves in rectangle.

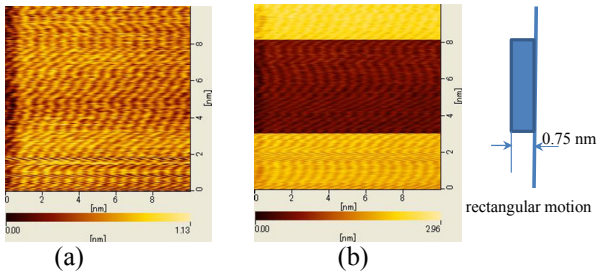

Fig.7. Mica AFM images observed by shape mode when the specimen table moved in rectangle. a) without rectangular motion, b) with rectangular motion.

4. CONCLUSIONS

To realize the displacement of less than one nanometer, we developed a reduction mechanism that can be mounted on an AFM instrument using the torsion leaf spring hinges, and demonstrated the sub-nanometer displacement with capacitance sensors and AFM images. The obtained results are as follows:

1) AFM mountable displacement reduction table was developed that can reduce the input displacement to 1/165, designed rate 1/180, at the specimen table totally.

2) The static and dynamic characteristics were investigated using an extension beam and capacitance sensors. It had the capability of generating the displacement of 0.73 nm, which corresponds to 0.1 nm at the specimen table. The reduction table had the natural frequency around 350 Hz.

3) Although the clear AFM atomic images could not be observed for the mica on the reduction table, probably because the thermal fluctuation and the natural vibration were too large to create the image, the diagonal atomic spacing was obtained as 0.45 nm.

Furthermore, an AFM atomic image can be shifted by the rectangle motion of the specimen table.

ACKNOWLEDGMENT

Partial financial support of the Scientific Research Fund of the Japanese Ministry of Education, Culture, Sports and Technology is gratefully acknowledged.

REFERENCES

[1] Nakata, T., and Watanabe, M. (2009). Ultracompact and highly sensitive common-path phase-shifting interferometer using photonic crystal polarizers as a reference mirror and a phase shifter. *Applied Optics*, Vol. 48, Issue 7, pp. 1322-1327.

[2] Aketagawa, M., Honda, H., Ishige, M. and Patamaporn, C. (2007). Two-dimensional encoder with picometer resolution using lattice spacing on regular crystalline surface as standard. *Meas. Sci. Technol.* Vol. 18, pp. 342–349.

[3] Gao, W., Araki, T., Kiyono, S., Okazaki, Y. and Yamanaka, M. (2003). Precision nano-fabrication and evaluation of a large area sinusoidal grid surface for a surface encoder. *Precis. Eng*. Vol. 27, pp. 289-298.

[4] Chen, TX., Koenders, L., Holger, Wolff, H., Neddermeyer, H. and Haertig, F. (2011) Atomic force microscope cantilevers as encoders for real-time forward and backward displacement measurements. *Meas. Sci. Technol.*, Vol. 22 094017 (12pp).

[5] Hayashi, M. and Fukuda, M. (2012) Generation of Nanometer Displacement using Reduction Mechanism Consisting of Torsional Leaf Spring Hinges. *Int. J. of Precision Engineering and Manufacturing*, Vol. 13, No. 5, pp. 679-684.

[6] AFM instrument: S-image by Hitachi High-Tech Science Corporation. (2013) http://www.hitachi-hitec-science. com/en/products/spm/S-image.html.

[7] Piezoelectric actuator: P-841.10 by Physik Instrumente (PI) GmbH & Co. (2013) http://www.physik-instrumente.com/en/pdf/P840/Datasheet.pdf.

[8] Thibaudau, F., Cousty, J., Balanzat, E., and Bouffard, S. (1991) Atomic-Force-Microscopy Observations of Tracks Induced by Swift Kr Ions in Mica. *Physical review letters*, Vol. 67, No. 12, pp. 1582-1585.

Received November 11, 2013.
Accepted February 3, 2014.